ChemElectroChem

Research Article
doi.org/10.1002/celc.202400273

Chemistry Europe
European Chemical Societies Publishing

www.chemelectrochem.org

Unraveling the Electron Transfer in *Cupriavidus necator* – Insights Into Mediator Reduction Mechanics

André Gemünde,[a] Nils-Lennart Ruppert,[a] and Dirk Holtmann*[a, b]

Cupriavidus necator, despite lacking direct electron transfer capabilities, demonstrates efficient reduction of various redox mediators in oxygen-free cultivation within bioelectrochemical systems. This study investigates the reduction site of ferricyanide through inhibition and expression rate analysis of oxygen and nitrate respiration chain complexes, comparing aerobic cultivation conditions with fructose as carbon and electron donor to autotrophic (CO_2/H_2/O_2) and anodic cultivation conditions (fructose/anode). Azide inhibition identified cytochrome c oxidase as the primary complex facilitating electron transfer to ferricyanide, with a secondary role proposed for nitrite reductase NirS, demonstrating a 3.9 ± 1.1-fold higher expression when exposed to anodic conditions. The 2.9 ± 0.6-fold increase in the expression of the natural porin OmpA under anodic conditions implies its potential involvement in ferricyanide uptake. Additionally, chemically permeabilizing cell membranes with cetyltrimethylammonium bromide doubles ferricyanide reduction rates without an anode present, offering insights for optimizing redox mediation in *C. necator* based bioelectrochemical systems. This study opens up new possibilities for the targeted optimization of mediated electron transfer in *C. necator* and other organisms.

Introduction

To develop sustainable biotechnological applications, the utilization of microorganisms capable of efficient CO_2 conversion has raised immense interest. Among these, *Cupriavidus necator* emerged as a promising strain for chemolithoautotrophic and chemoorganotrophic cultivation, demonstrating its potential as a capable producer of polyhydroxyalkanoates as biological polymer alternative,[1] terpenes as a basis for fragrances and advanced biofuels,[2–4] precursors for aroma components like ferulic acid,[5] and branched-chain alcohols (isobutanol and 3-methyl-1-butanol) as alternative biofuels.[6] The genetic accessibility further allows for even more products to be integrated for industrial-scale production.[7] When fed with CO_2 and H_2, *C. necator* is able to fix the carbon through the Calvin-Benson-Bassham cycle and acquires electrons through the oxidation of H_2 via its soluble hydrogenase. On the electron acceptor side, *C. necator* proves to be respiratory flexible, as it can naturally rely on two different terminal electron acceptors, NO_3^- and O_2. However, with NO_3^- as the terminal electron acceptor, the growth rate is greatly reduced.[8] Most of the nitrate respiration as well as the hydrogen oxidation genes are located on the pHG1 megaplasmid. The pHG1 plasmid further contains 429 potential genes including the CO_2 fixation enzymes and cytochrome c maturation genes.[9] While the prospects of utilizing this strain in chemolithoautotrophic cultivation systems for CO_2 fixation and industrial-scale production are encouraging, challenges persist, particularly concerning explosion risks of H_2/O_2 gas mixtures and operation costs from O_2 transfer into the cultivation medium. With the use of microbial electrochemical technologies, these challenges might be addressed through anodic electron discharge. Hereby, an anode offers the possibility to act as terminal and inexhaustible electron acceptor for *C. necator* instead of O_2.

However, one major obstacle when using bioelectrochemical systems often lies in the lack of a detailed understanding of the electron transfer mechanisms. This also applies to *C. necator*. The proteome of *C. necator* provides no known genes enabling a direct extracellular electron transfer (DET). Nevertheless, using a mediated extracellular electron transfer (MET), electron transfer between planktonic cells and an electrode can still be established. It has already been recognized, that *C. necator* can interact with ferricyanide and various other mediators.[10–13] The specific interaction site that engages with ferricyanide or any other mediator in *C. necator* still remains unclear. The MET process has further been demonstrated with the polymeric redox mediator poly(2-methacryloyloxyethyl phosphorylcholine-co-vinylferrocene) in the presence of oxygen as the main electron acceptor.[10] Here, an upregulation of three nitrate reductases was detected, indicating their potential role in MET. Another study used neutral red to supply electrons in the opposite direction from a cathode to *C. necator*,[11] but the study lacks a clear definition of the mediator interaction site.

The determination of the interaction sites for various redox mediators in other organisms has yet been challenging. So far,

[a] A. Gemünde, N.-L. Ruppert, Prof. D. Holtmann
Institute of Bioprocess Engineering and Pharmaceutical Technology and Competence Centre for Sustainable Engineering and Environmental Systems
University of Applied Sciences Mittelhessen
35390 Giessen, Germany

[b] Prof. D. Holtmann
Institute of Process Engineering in Life Sciences
Karlsruhe Institute of Technology
76131 Karlsruhe, Germany
E-mail: dirk.holtmann@kit.edu

Supporting information for this article is available on the WWW under https://doi.org/10.1002/celc.202400273

inhibition results with antimycin A and azide hint towards cytochrome c reductase as the interaction site of the mediators ferricyanide and tris(2,2′-bipyridyl)cobalt(III) in *Pseudomonas putida* KT2440.[14] In *Lactococcus lactis*, the endogenous mediator 2-amino-3-carboxy-1,4-naphthoquinone accepts electrons from the type II NADH dehydrogenase (NoxAB) which then reduces ferricyanide in the periplasm or extracellular.[15] Adding to the complexity, various mediators may interact with different interaction sites. As an example, the lipophilic compound 2,6-dichlorphenolindophenol (DCIP) can accept electrons directly from complex I of the respiration chain in *Staphylococcus aureus*,[16] while neutral red can penetrate both membranes and most likely reduces NAD^+ directly in the cytosol.[17]

In *C. necator*, the so far reached current densities via MET are insufficient to replace O_2 entirely.[12] Therefore, methods to enhance mediator reduction rates are needed. A significant bottleneck for MET is the cell membrane itself. Theoretically, its lipophilic characteristics pose a disadvantage for numerous hydrophilic or charged mediators, preventing their passage. However, it has been demonstrated, that some hydrophilic redox mediators, like ferricyanide,[14,18] can penetrate the outer membrane of Gram-negative bacteria while lipophilic mediators can most likely pass both membranes.[19] The uptake mechanisms are still barely known and further research is needed. It is conceivable though, that outer membrane porins, like OmpF in *P. putida*, play an important role in the uptake of hydrophilic, charged mediators.[18]

In this context, our study aims to elucidate the interaction sites of ferricyanide within *C. necator* using fructose as electron and carbon donor and an anode as the only available terminal electron acceptor. Hypothesized interaction sites are narrowed down through inhibition studies, qPCR analysis, and the use of a pHG1 megaplasmid deficient strain (Illustrated in Scheme 1). Additionally, our objective is to optimize MET by increasing mediator membrane transfer as a potential bottleneck. In this preliminary investigation, our research is focused on understanding the involvement of key cellular components in MET, particularly in the context of ferricyanide reduction. Additionally, our study explored the permeabilization of cellular membranes to gain insights into potential strategies for enhancing electron transfer efficiency

Results and Discussion

Reduction of Ferricyanide in a BES

In this study, a BES reactor system with ferricyanide as a redox mediator was used to elucidate the mediated electron transfer mechanisms within *C. necator*. A PHB deficient strain (*C. necator* PHB^-) was used primarily to eliminate side effects from stored metabolic reserves. As a benchmark with 5 mM ferricyanide and an anode poised at 500 mV *vs.* Ag/AgCl (satd. KCl), *C. necator* PHB^- reached a maximum current density of $183 \pm 5\ \mu A\,cm^{-2}$ and a total charge of 1686 ± 101 C was transferred within 192 h

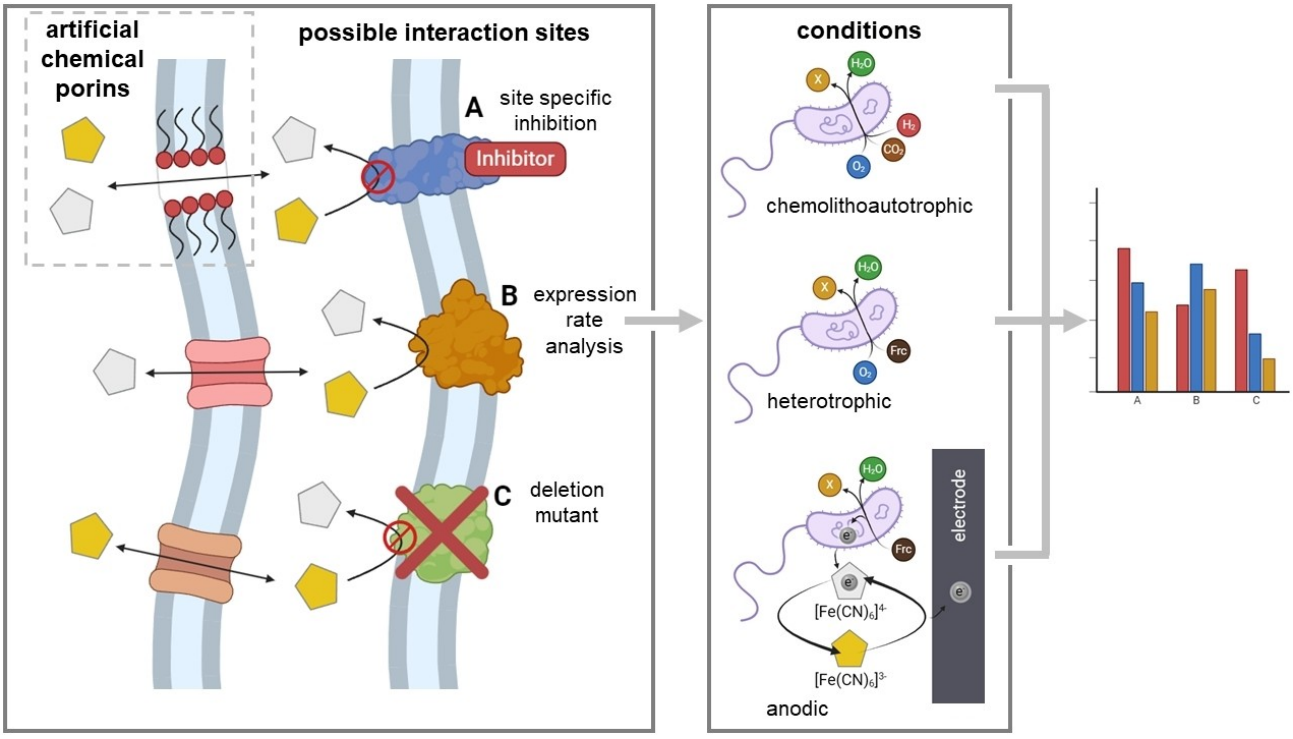

Scheme 1. Illustration of the aims of the study. Possible interaction sites of ferricyanide (pentagons, yellow: oxidized, grey: reduced) within *C. necator* are narrowed down via specific inhibition, applying deletion mutants, and expression rate analysis comparing chemolithoautotrophic, heterotrophic, and anodic cultivation conditions. Furthermore, the influence of creating artificial porins with chemical permeabilizers on anodic electron transfer is studied. Created with BioRender.

(Figure 1a). While the current density increases, the ΔOD_{600} rises slightly from 1.2 (0 h) to 1.7 after 6 h. The cell density remains almost constant for the rest of the cultivation period. The total fructose consumption is only $0.3 \pm 0.02\ g\,L^{-1}$ (Figure 1b). The electrons originating from fructose are transferred through ferricyanide to the anode at a coulombic efficiency of $63.1 \pm 5.7\%$, with no side products detectable by HPLC analysis. The remaining fraction of electrons could, in theory, be disposed of through the bidirectional soluble hydrogenase, generating gaseous H_2.[20] A further option would be the conversion into biomass, hence the observed growth within the first 6 h. Most of the oxidized ferricyanide is also reduced within the first 6 h, while the current rises. The maximum mediator reduction rate in this phase reached $0.22\ mM\,h^{-1}$. As the current drops over time, the ratio of oxidized to reduced ferricyanide tends towards the oxidized state. It seems likely, that *C. necator* is not able to support the high initial current and reduction rate over extended time periods. Limitations can be assumed within the metabolism and the mediator transfer-rate, since the anode provides enough oxidized ferricyanide in the bulk medium to keep up the electron transfer from *C. necator* to the anode (Figure 1a, red squares).

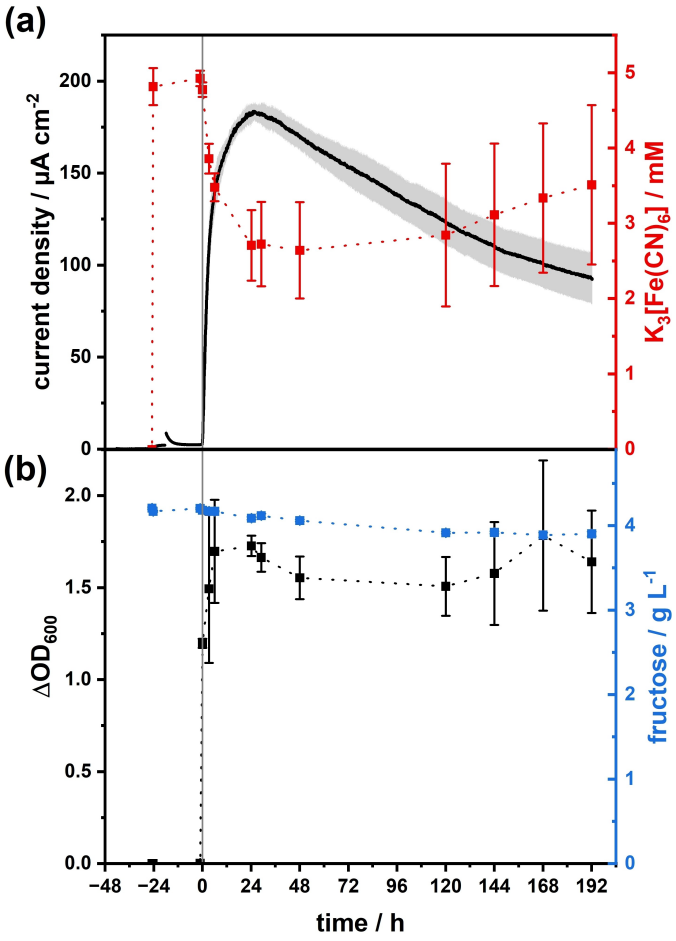

Figure 1. *C. necator* reference BES cultivation with 5 mM ferricyanide as mediator. (a) Current density (black line) and concentration of oxidized ferricyanide (red) from a biological triplicate. (b) cell density determined via ΔOD_{600} (black squares) measurement and fructose concentration (blue) during cultivation. Conditions: MMasy minimal medium, 30 °C, 400 rpm, pH = 6.8, n = 3, 500 mV *vs.* Ag/AgCl (satd. KCl). Error bars depict the standard deviation.

Expression Rate Analysis within BES Cultures

To get a deeper understanding of the MET mechanism, the first step is to shed some light on the interaction site of ferricyanide with *C. necator*. So far, it can be assumed that *C. necator* is unable to transfer electrons directly to an anode, as control experiments without ferricyanide as a mediator in the BES show no current evolution (Figure S1). It is therefore most likely, that no electron-transferring cytochromes are located on the outer membrane, as it is known for *Geobacter sulfurreducens*, *Shewanella oneidensis*, or *Vibrio natriegens*.[21–23] The interaction site is therefore expected to be located on the cytoplasmic membrane, or in the cytosol. Cytosolic sites are excluded in this study since ferricyanide is most likely not able to reach the cytosol.[24]

Therefore, several hypothesized interaction sites that are located on the cytoplasmic membrane or in the periplasmic space (Table S1) were chosen for expression rate analysis by qPCR. Of these interaction sites, one group comprises the respiration chain complexes (Figure 2a), another group includes both the soluble and membrane-bound hydrogenases together with three channel proteins (OmpA, ImpK, czcC2), which might be involved in the outer-membrane transfer of ferricyanide (Figure 2b). Additionally, the nitrate respiration proteins were chosen for analysis (Figure 2c), since the interaction of nitrate reductase with ferricyanide has already been suggested in *E. coli*.[24] Expression rates for all identified interaction sites were compared to stationary aerobic cultures (48 h after inoculation) without ferricyanide in a shake flask. Cultivation conditions to compare were stationary (54 h) autotrophic cultures on $CO_2/H_2/O_2$ and BES cultures with ferricyanide and the anode as a terminal electron acceptor. Samples from BES cultures were taken 24 h after inoculation, where current densities peaked. Within the BES cultivation, a specific mutant lacking the pHG1 megaplasmid (*C. necator* ΔpHG1) was chosen as negative control for qPCR analysis. Via this control, the missing interaction sites from the pHG1 megaplasmid and their relevance for MET can be elucidated. The relative gene expression rates for autotrophic cultivation, BES cultivation and the ΔpHG1 strain *vs.* aerobic conditions as reference were determined via the $2^{-\Delta\Delta Ct}$ method.

From the relative expression rates gathered, it can be concluded that the respiration chain proteins are not over-expressed significantly under BES conditions. One exception is the cytochrome c oxidase (cbb3) with a relative expression *vs.* aerobic conditions of 1.9 ± 0.3 in a BES. Slightly higher expression rates were determined for autotrophically grown cells with values ranging from 1.2 ± 0.1-fold for cytochrome c reductase to 1.9 ± 0.1-fold for the ATPase (Figure 2a). The pHG1 deficient strain expresses the respiration chain complexes within the same range (minding the error) as the pHG1 containing strain.

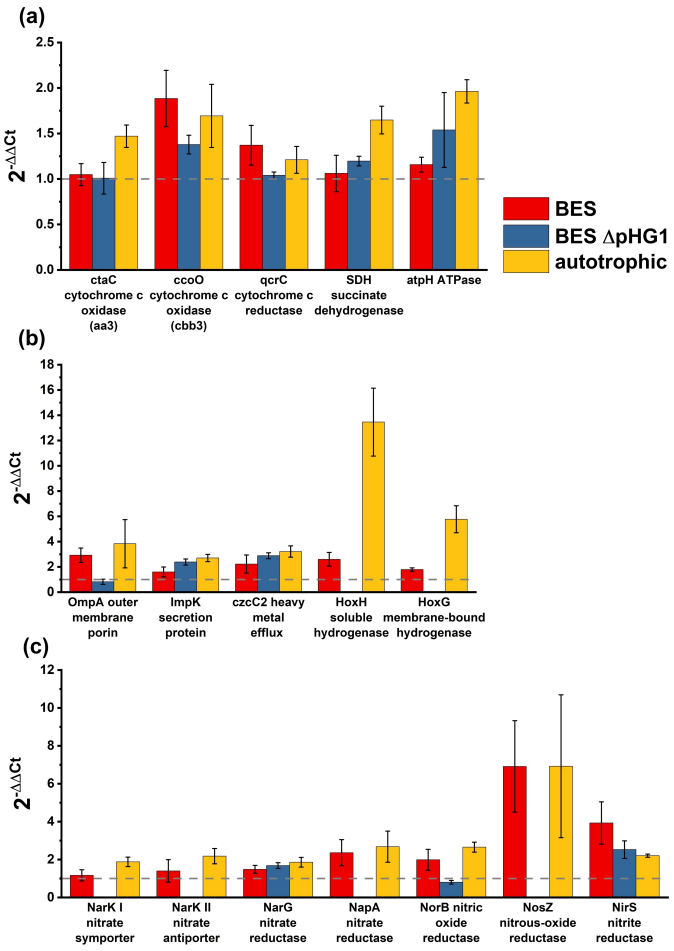

Figure 2. Relative gene expression levels in BES and autotrophic cultures of hypothesized proteins involved in the MET process *vs.* stationary aerobic culture as calibrator. BES samples were taken from the reactor 24 h after inoculation. Autotrophic samples were cultivated until stationary (54 h). (GyrB (pos. control, housekeeping; CtaC (aa3-type cytochrome oxidase, subunit II), CcoO (cbb3-type cytochrome oxidase, monohaem subunit II), GcrC (ubiquinol-cytochrome c reductase, cytochrome c1), SDH (succinate dehydrogenase iron-sulfur subunit), NuoD (NADH-quinone oxidoreductase subunit D), AtpH (F-type H+-transporting ATPase subunit delta, NarK I (nitrate/proton symporter), NarK II (nitrate/nitrite antiporter), NarG (respiratory nitrate reductase catalytic subunit), NapA (periplasmic nitrate reductase large subunit), NorB (nitric oxide reductase subunit B), NosZ (nitrous-oxide reductase), NirS (cytochrome cd1 nitrite reductase), OmpA (outer membrane protein or related peptidoglycan-associated (lipo)protein), ImpK (type VI secretion system protein), CzcC2 (outer membrane protein, heavy metal efflux system). Error bars depict the standard deviation.

From the three porins chosen for qPCR analysis, OmpA is expressed 2.9 ± 0.6 and 3.8 ± 1.9-fold higher under both anaerobic conditions (BES and autotrophic) compared to aerobic cultivation. This seems to be independent of the anodic conditions. Contrary to that, the expression in the ΔpHG1 strain under BES conditions is comparable to aerobic conditions, even though OmpA is encoded on chromosome 1, rather than the pHG1 plasmid. In a broader context, OmpA proteins are characterized by an N-terminal domain that configures an eight-stranded, antiparallel β barrel embedded within the outer membrane.[25] The globular C-terminal domain of OmpA is situated within the periplasmic space. Outer membrane proteins in Gram-negative bacteria serve diverse functions, e.g., signal transduction, adhesion to host cells, catalysis of crucial reactions, and facilitation of active and passive transport of solutes and nutrients across the cell membrane.[26] This may enable the MET in the first place, by importing and exporting ferricyanide.

The two other efflux proteins are expressed by a factor of 1.6 ± 0.4 (ImpK) and 2.2 ± 0.7 (czcC2) in a BES with pHG1. Since the expression is even higher within the ΔpHG1 strain in BES and autotrophic cultures, the effect is most probably triggered by the lack of O_2. ImpK is a primarily inner membrane protein with a C-terminal OmpA-like domain facing the periplasm. However, a small fraction of the total ImpK amount was also located in the outer membrane of Gram-negative *Agrobacterium tumefaciens*.[27] The protein is associated with the bacterial type VI secretion system providing a membrane channel with a pore size of 40 Å,[28] large enough for small molecules like ferricyanide to pass. CzcC is equally an efflux protein complex, transporting divalent cations through the outer membrane as a proton antiporter.[29] A passive or active import of ferricyanide via one of the two complexes cannot be proven by qPCR and might be unlikely when looking into the mechanisms, but cannot be ruled out. Further research in mediator membrane transport will be needed to shed light on the exact mechanism(s).

As expected, both the soluble (SH) and membrane-bound hydrogenases (MBH) are not expressed when the pHG1 plasmid is absent and significantly over-expressed under autotrophic cultivation conditions with hydrogen present (5.8 ± 1.1 times for MBH and 13.5 ± 2.7 times for SH). Within the BES, these hydrogenases can be found at expression rates of 2.6 ± 0.5-fold higher for SH and 1.8 ± 0.1-fold higher for MBH in comparison to aerobic conditions. These hydrogenases are reportedly only expressed under autotrophic conditions feeding on $H_2/CO_2/O_2$ gas mixtures as well as under heterotrophic conditions with a switch from fructose to the less favourable substrate glycerol.[30,31] Based on our results, it can be concluded that these hydrogenases are expressed under BES conditions, but to a very limited extent.

The obtained data from the denitrification pathway proteins supports the conclusion that both the membrane-bound nitrate reductase (NarG) and periplasmic nitrate reductase (NapA) are expressed under BES conditions (1.5 ± 0.2 and 2.4 ± 0.7 respectively), similar to autotrophic cultivation conditions (1.9 ± 0.3 and 2.7 ± 0.8). These enzymes catalyse the first step in denitrification ($NO_3 \rightarrow NO_2$, $E^0 = 420$ mV),[32] when nitrate is available as an electron acceptor. It has to be noted, that the present minimal medium only contains ammonium sulphate as a nitrogen source. It is known, that NarG only forms in the absence of O_2, while NapA forms in the stationary phase of growth under aerobic conditions.[32] Therefore, NapA is already present from the stationary pre-culture when *C. necator* is added to the BES. Furthermore, the NapA genes are located on the pHG1 megaplasmid, hence it is not expressed in the ΔpHG1 BES cultivation. The proven expression in a BES together with the accessibility from the periplasm and standard redox potential of 420 mV of these reductases makes the reduction of

ferricyanide theoretically feasible (E^0 = 416 mV *vs.* SHE for ferricyanide).[33] It has to be considered though, that ferricyanide might mimic oxygen in a way, that the oxidizing conditions within the culture broth may inhibit the nitrate reduction pathway during the cultivation.[34]

Periplasmic nitrite reductase (NirS) converts NO_2 into the toxic intermediate NO. Regarding the redox potential, the reaction with ferricyanide is feasible, since the NO_2/NO reaction couple exhibits an E^0 of 375 mV *vs.* SHE.[32] In Figure 2c, NirS is expressed 3.9 ± 1.1-fold in a BES *vs.* 2.2 ± 0.1-fold with H_2/CO_2/O_2. This reductase is encoded on the chromosome, hence the expression is also measurable 2.5 ± 0.5-fold with the pHG1 deficient strain. The nitric oxide reductase (Nor) catalyses the reaction of NO→N_2O (E^0 = 1175 mV).[32] The necessary genes are located in two copies, one on the pHG1 megaplasmid and one on the chromosome.[35] From our data, this is visible in the expression rate of NorB. The difference between autotrophic and BES cultivation is marginal (2.0 ± 0.6 *vs.* 2.7 ± 0.3) with respect to the error. The ΔpHG1 strain expresses NorB 0.8 ± 0.1-times the amount that an aerobically grown strain with the pHG1 plasmid achieves. The NorB subunit contains two *b*-type hemes, but no heme *c*. The enzyme was also able to accept electrons from reduced phenazine methosulfate (E^0 = 80 mV *vs.* SHE) .[36,37] If the enzyme is also able to reduce ferricyanide is speculative, since the redox potential of the catalysed reaction might be too high compared to the E^0 of ferricyanide.

The nitrous-oxide reductase (NosZ) catalyses the last step from N_2O→N_2 (E^0 = 1335 mV).[32] For this specific site, the expression rate was equal for autotrophic and BES conditions with a 6.9-fold higher rate. It has to be noted though, that standard deviations were uncommonly high. Both NarK nitrate transport proteins were not significantly over-expressed with ferricyanide in a BES. Their involvement in ferricyanide import is not yet determined. The fact that these transporters are naturally importing anions might benefit the ferricyanide uptake. However, there is evidence for a reversible inactivation of NarK under oxidizing conditions, which in turn, stops the transport.[38] The nitrate assimilatory enzyme (Nas) is inhibited by ammonium, which is always present in the medium.[39] Therefore, it was not part of the analysis. To summarize, both nitrate reductases (NapA and NarG) expose reachable interaction sites for ferricyanide in the periplasm and the reduction is thermodynamically feasible. The same applies for the nitrite reductase (NirS).

Eliminating Megaplasmid Encoded Interaction Sites

The role of the nitrite/nitrate reductases and both hydrogenases in MET cannot be concluded via qPCR alone. Therefore, BES data comparing the ΔpHG1 *vs.* the PHB^- strain can shed light on their role in MET. The pHG1 megaplasmid contains all hydrogenases, including the regulatory and actinobacterial hydrogenases,[7] as well as most of the nitrate respiration genes (Table S1). With those possible interaction sites missing, as it was confirmed via qPCR, no current response should be possible with this strain if one of the missing genes plays a crucial role in ferricyanide reduction.

Figure 3a shows the result for a BES cultivation of the ΔpHG1 strain with ferricyanide in a biological triplicate. The black line indicates the current density increasing right after inoculation at t = 0 h. As for the control with the PHB^- strain (Figure 1), the current density for the ΔpHG1 strain reaches a slightly lower maximum of 161 ± 14 μA cm^{-2} and a similar coulombic efficiency of 68.1 ± 9%. Even without the soluble and membrane-bound hydrogenase, a part of the electrons is not transferred to the anode, ruling out the theory of H_2 production through the hydrogenases. Ferricyanide (red squares) is reduced at the highest rate (0.19 mM h^{-1}) during the initial phase when the current rises after inoculation, as observed before with *C. necator* PHB^-. With the current density reaching a plateau, the reduction rate of *C. necator* seems to be equal to the re-oxidation rate by the anode. Hence, the concentration of oxidized ferricyanide stays nearly constant. When the current starts to decline, the equilibrium shifts

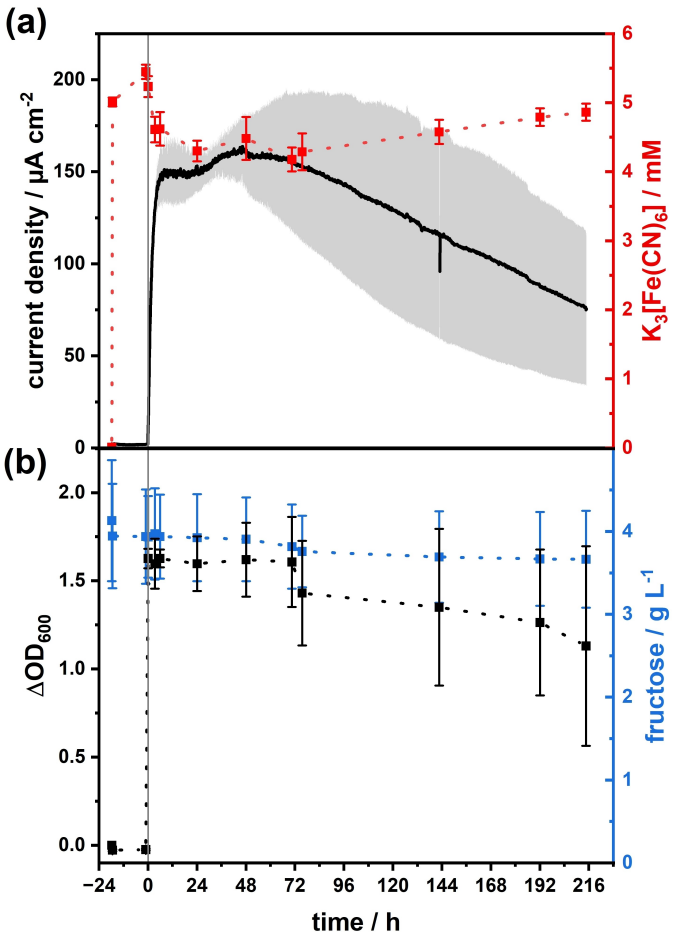

Figure 3. BES cultivation of *C. necator* HF210 strain, lacking the pHG1 megaplasmid. (a) Current density (black) and concentration of oxidized ferricyanide (red) from a biological triplicate. (b) cell density determined via ΔOD_{600} (black squares) measurement and fructose concentration (blue) during cultivation. Conditions: MMasy minimal medium, 30 °C, 400 rpm, pH 6.8, n = 3, 500 mV *vs.* Ag/AgCl (satd. KCl). Error bars depict the standard deviation.

towards the anode re-oxidizing ferricyanide, so the concentration starts to rise to the originally added value.

Figure 3b depicts the cell density as ΔOD_{600} values. In contrast to the PHB^- strain, the ΔOD_{600} doesn't increase within the first 6 h of cultivation. However, both strains share the low fructose uptake in a BES cultivation, with the ΔpHG1 strain consuming $0.27 \pm 0.02\ g\,L^{-1}$ of fructose during 216 h of cultivation. The overall standard deviations were significantly higher with the ΔpHG1 strain. This originates from reactor cultures varying in ΔOD_{600}, current density, and total fructose concentration, although stemming from parallel pre-cultures and using one identical medium stock.

In summary, the current density in the ΔpHG1 strain follows the same pattern as observed in the strain containing the pHG1 plasmid. This observation rules out all hydrogenases and the nitrate respiration pathway, except membrane-bound nitrate (NarG) and nitrite (NirS) reductases which are also located on the chromosome, as the main interaction site for ferricyanide.

Inhibition of Suspected Interaction Sites

A common method for identifying interaction sites is specific inhibition. By applying inhibitors of the respiration chain complexes and the nitrate reductases during BES cultivation of *C. necator*, the effects of site-specific inhibition on the current generation and redox state of ferricyanide can be studied. The specific inhibition site, the postulated inhibition mechanism, and the applied concentration of each substance used in this study are listed in Table 1. The resilience of *C. necator* against the inhibitors was determined via growth analysis in aerobic cultivation. In the end, the concentration where growth is inhibited but no rapid cell death occurs was chosen for BES experiments (data not shown). Myxothiazol and rotenone are poorly soluble in aqueous buffers leading to increased turbidity, hence the OD values become more uncertain.

The applied inhibitors listed in Table 1 were added within the stable/declining current phase, so the effect of each inhibitor is visible. The current density plots and the respective concentrations of ferricyanide are plotted in Figure 4. The associated ΔOD_{600} values are plotted in the supplementary information (Figure S2).

The inhibition of cytochrome c reductase with antimycin A affects the current response from *C. necator* in the BES immediately (Figure 4a). As antimycin A is introduced into the reactor, the current density drops fast. The reduced ferricyanide is not re-oxidized by the anode as the current declines, indicating an interaction of antimycin A with the electrode or ferricyanide itself, preventing the oxidation. It cannot be ruled out, that this side reaction causes the observed drop in current density, rather than the inhibition itself. The same effect was observed for *C. necator* ΔpHG1 (Figure S3) and was also demonstrated by Lai and co-workers in their BES with *P. putida*.[14] Antimycin A blocks the quinone reduction from Q to QH_2 at the Q_i site of cytochrome c reductase (Table 1). Nevertheless, if ferricyanide is reduced at the Q_0 site, where QH_2 is oxidized back to Q, antimycin A would not directly interfere with this reaction. Ferricyanide reduction could therefore continue until the QH_2-pool is deprived and the insufficient proton gradient starves ATP synthesis. The inhibition of the antimycin A insensitive Q_0 site with myxothiazol, however, had no effect on the current density with 6.8 μM of the inhibitor added into the culture (Figure 4b). It is conceivable though, that the inhibitor concentration might be too low, due to the poor solubility, to effectively inhibit cytochrome c reductase. With the substantial number of cells in the reactor, the inhibition of only a few cytochrome c reductase enzymes would therefore not affect the current density curve. Because of the unclear way antimycin A interacts with ferricyanide or the electrode and the fact that myxothiazol doesn't dissolve well, we can't say for sure if cytochrome c reductase is an important site for ferricyanide interaction.

Table 1. Inhibitors used in this study with their respective interaction sites and known inhibition mechanism.

Inhibitor	Inhibition site	Inhibition mechanism	Concentration used
Antimycin A	Cytochrome c reductase Q_i site	Blocks quinone reduction site (Q_i) of the bc_1 complex near heme b_H, preventing generation of the semiquinone in the second half of the Q-cycle.[40]	20 $\mu g\,mL^{-1}$
Myxothiazol	Cytochrome c reductase Q_0 site	Blocks Fe–S oxidation of ubiquinol at Q_o site.[41]	6.8 μM
Rotenone	NADH dehydrogenase	Inhibition of last electron transfer step from Fe–S cluster to ubiquinone.[42] Side effect: generation of reactive oxygen species leading to apoptosis.[43]	200 μM
	Nitrate reduction	Unknown[44]	
Sodium azide	Cytochrome c oxidase	Binding between heme a_3 and Cu_B in O_2 reduction site.[45] Side effect: ATP hydrolase activity of the ATPase is inhibited.[46]	5 mM
	Nitrate reductases (Nar, Nap)	Unknown. Nar is sensitive to azide in the μM, Nap in the mM range.[47,48]	
$ZnSO_4$	Periplasmic nitrate reductase (NapA)	Uncompetitive, Zn^{2+} binding site (sulphur or methionyl residue of methionine 153) is revealed when nitrate is bound.[49]	400 μM
Malonate	Succinate dehydrogenase	Unknown.[50]	20 mM

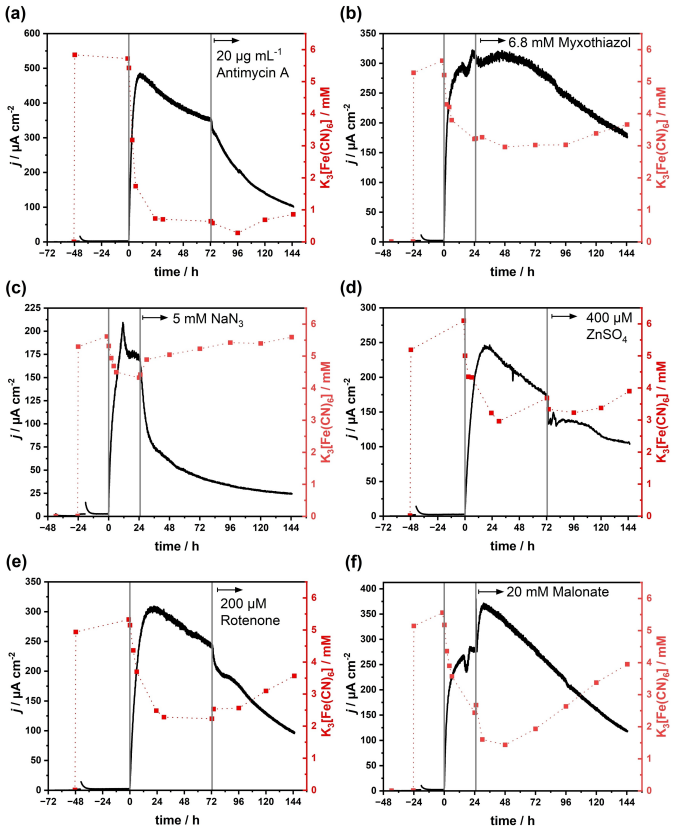

Figure 4. Inhibition studies with *C. necator* BES cultures containing 5 mM ferricyanide as mediator. Inhibition: (a) cytochrome c reductase Q_i site with 20 µg mL^{-1} antimycin A, (b) cytochrome c reductase Q_o site with 6.8 µM myxothiazol, (c) cytochrome c oxidase with 5 mM sodium azide, (d) periplasmic nitrate reductase with 400 µM zinc sulphate, (e) NADH dehydrogenase with 200 µM rotenone, (f) succinate dehydrogenase with 20 mM malonate. Current density (black) and concentration of oxidized ferricyanide (red). Conditions: MMasy minimal medium, 30 °C, 400 rpm, pH 6.8, 500 mV *vs.* Ag/AgCl (satd. KCl). Cell densities measured via ΔOD_{600} can be found in Figure S2.

The addition of 5 mM sodium azide (Figure 4c) led to an immediate drop in current density with simultaneous re-oxidation of ferricyanide. Contrary, in experiments conducted with *P. putida* F1, no current changes were observed when cytochrome c oxidase was inhibited with 3 mM sodium azide.[14] It's important to note that the reduction of the mediator follows a similar pattern to the control experiment: as the current density decreases, the concentration of oxidized mediator increases. In contrast to the inhibition with antimycin A, this demonstrates that ferricyanide and the electrode are not affected by azide. Furthermore, the cell density measured by ΔOD_{600} doesn't decrease significantly in the first 24 h following the addition of azide (Figure S2b), indicating the current decline is not a result of cell lysis. Studies in *E. coli* could demonstrate, that 6 mM of potassium cyanide added to mid-exponential cells limits the ferricyanide reductase activity of cytochrome c oxidase to 14 %.[51] In our experiment with stationary cells, the current response, which indicates reductase activity, decreased from 170 µA cm^{-2} to 24 µA cm^{-2} (and continued to decline slightly) within 120 h after adding azide, representing approximately 14 % of the initial current remaining.

Mechanistically, cytochrome c oxidase catalyses oxygen reduction between cytochrome a_3 and the Cu_B site, accessible for oxygen located in the cytoplasmic membrane.[52] Interrupting the electron transfer chain at cytochrome c oxidase would lead to the over-reduction of chain components upstream. However, since molecular oxygen is excluded from the medium, no reactive oxygen species should result from this effect. Most importantly, inhibiting the oxygen reduction site with azide would have no effect on ferricyanide reduction, if the mediator cannot access the a_3/Cu_B binuclear site. This is likely the case, since the charged molecule will not penetrate the cytoplasmic membrane. This indicates, that $[Fe(CN)_6]^{3-}$ can't replace oxygen within the normal catalytic cycle of cytochrome c oxidase. Nevertheless, reduced $[Fe(CN)_6]^{4-}$ can likely donate electrons to cytochrome c oxidase through the Cu_A site, accessible from the periplasm.[53] Studies with isolated cytochrome c oxidase placed in liposomes further suggested that the oxidized $[Fe(CN)_6]^{3-}$ can be reduced at the cytochrome c reduction site via Cu_A and heme a.[54] If this mechanism results in a proton translocation, e.g., via the release of redox Bohr protons, remains speculative.[55]

It has to be considered though, that azide concentrations in the mM range will also inhibit both nitrate reductases Nar and Nap (Table 1). The pHG1 deficient strain, which lacks NapA and still effectively reduces ferricyanide, rules out NapA as a possible interaction site for ferricyanide. This suggests that NarG could be an alternative active site for ferricyanide reduction, distinct from cytochrome c oxidase. The 14 % leftover current after inhibition suggests that the nitrite reductase NirS might be responsible for maintaining the remaining anodic electron transfer.

As a control, the periplasmic nitrate reductase (Nap) was inhibited with 400 µM of $ZnSO_4$, which resulted in an instant decline in current by 40 µA cm^{-2} before reaching a plateau and proceeding with the initial decline, 36 h after inhibition (Figure 4d). Ferricyanide seems to be recovered as expected while the ΔOD_{600} increases rapidly from 1.16 to 1.69 and stabilizes over the next 72 h at about 1.5. This sudden increase can only be explained by adsorbed cells being resuspended again since $ZnSO_4$ doesn't absorb at 600 nm. Hence, the inhibition of the periplasmic nitrate reductase (NapA) doesn't seem to affect the MET in great effect, validating the previously discussed results.

The inhibition of NADH dehydrogenase with rotenone (Figure 4e) led to a similar observation as the inhibition with $ZnSO_4$. After adding the inhibitor, the current density drops by 50 µA cm^{-2}, then reaches a plateau before continuing to decline as observed before the inhibition. Additionally, ferricyanide undergoes rapid oxidation during the decline in current. Afterwards, the ferricyanide concentration mirrors the current density curve, as observed in the control experiment (Figure 1). Similar results were observed with 250 µM of rotenone in *P. putida* F1,[14] leading to the assumption that NADH dehydrogenase is not a reduction site for ferricyanide.

Finally, 20 mM malonate was used to inhibit succinate dehydrogenase. The briefly occurring pH drop caused by the addition of malonic acid resulted in a short current spike, which was quickly recovered by the pH control unit (Figure 4f).

Interestingly, after inhibition, there was an initial increase in the current response along with a further reduction of ferricyanide. However, this effect is not stable, and the current density quickly decreases again. A reducing effect of malonate on ferricyanide was ruled out in abiotic tests over 24 h (data not shown). Moreover, a metabolic pathway utilizing malonic acid as a substrate is unknown for *C. necator*. A comprehensive justification explaining this effect cannot be provided in this context. Continued investigation into this observation may provide a pathway for optimizing MET.

While it is not possible to create a mutant strain lacking parts of the respiration chain, total RNA sequencing to compare expression levels for all available mRNA during BES cultivation might be a further option to identify the interaction sites of different mediators accurately. However, the azide inhibition performed in this study suggests that cytochrome c oxidase is the primary site of reduction for ferricyanide under BES conditions. This observation leads to similar conclusions as those stated by Ertl and Unterladstaetter[51] for *E. coli* and likely applies to other Gram-negative organisms as well: The rate of ferricyanide reduction ultimately depends on the expression rate of transport proteins and respiratory cytochrome c oxidase.

Overcoming the Membrane Obstacle

Since an artificial over-expression of the respiratory enzymes is not feasible, the first step in optimizing MET is to increase the membrane transfer rate of ferricyanide to circumvent a possible limitation.[56,57] This was initially addressed by expressing various porins in *C. necator* PHB$^-$. The heterologous expression of the FhuA porin from *E. coli* and its derivative missing the "cork" domain FhuA Δ1-160, along with the channel protein OprF from *Pseudomonas aeruginosa*, did not exhibit a positive impact on mediated electron transfer in *C. necator*. Contrarily, the metabolic burden associated with expressing these porins led to a reduction in current densities (Figure S4). However, our qPCR investigations suggest that the outer membrane protein OmpA may be involved in the artificial electron transfer process and should be further investigated.

Alternatively, we investigated cetyltrimethylammonium bromide (CTAB), benzalkonium chloride, EDTA, Triton X 100, polyethylenimine (PEI), Tween 20, and succimer (dimercaptosuccinic acid), as possible chemical permeabilizing agents. These substances are expected to create artificial pores in the outer (and potentially inner) membrane, to facilitate the membrane transfer of ferricyanide.[57–59] Toxic concentrations for the respective substances were determined via growth curves at increasing concentrations (Figure S5). Via an uptake assay of the fluorescent probe N-Phenyl-1-naphthylamine (NPN) *vs.* non-treated cells, increased membrane permeation could be demonstrated for succimer, PEI, benzalkonium chloride, and CTAB (Figure S6, Figure 5a). In contrast, EDTA, Triton-X-100, and Tween 20 could not increase the uptake of NPN (Figure S6). In a further step, the concentrations for effective membrane permeabilization and minimal cell toxicity were determined and prepared for reduction assays with ferricyanide. However, side reactions with the mediator like clumping, precipitation, increased turbidity, and reduction of ferricyanide prohibited the use of succimer, PEI, and benzalkonium chloride for BES cultivation (Figure S7). This issue might be resolved when other mediators are used. At last, only CTAB was compatible with ferricyanide, with a minimal turbidity increase with 20 μM CTAB.

Figure 5a depicts the NPN uptake with ascending CTAB concentrations. Increased emission rates *vs.* background therefore hint towards increased cell membrane permeation. Stepping up the CTAB concentration in the range of 20 to 300 μM doesn't result in higher fluorescence signals of NPN, indicating a concentration-independent mechanism for the number of cells applied within the well. However, a limiting amount of NPN cannot be ruled out.

In growth analysis experiments conducted in 96-well plates, *C. necator* could not replicate in CTAB containing growth medium (Figure 5b). For minimal medium with a starting ΔOD_{600} of 0.5 supplemented with 300 μM CTAB, a decrease in ΔOD_{600} suggests the maximum concentration for vital resting cells is 220 μM. As previously described, membrane permeability is not concentration-dependent. Therefore, a concentration of 20 μM CTAB was selected for BES experiments to minimize toxic stress on the cells. Preliminary experiments in anaerobic serum flasks with fructose as electron and carbon source and ferricyanide as the sole electron acceptor were performed to determine ferricyanide reduction rates. In comparison to non-permeabilized cells, CTAB treated cells with identical ΔOD_{600} values reduce ferricyanide 2-fold faster with 53 $\mu M\,h^{-1}$ *vs.* 27 $\mu M\,h^{-1}$ (Figure 5c, d).

A recent study by Wu and co-workers[58] applied CTAB to anaerobic sludge biofilms in a MFC with an optimum of 200 μM CTAB to facilitate riboflavin-mediated electron transfer. However, there are no studies yet about the actual application of CTAB using pure cultures within a BES. Hence, our objective was to enhance the MET process with *C. necator* by introducing 20 μM CTAB into the BES reactor. Additionally, the impact of artificial pores on fructose uptake is a subject of further investigation. Figure 6 depicts the recorded current densities with (red) and without (black) CTAB (Figure 6a) and the respective concentrations of oxidized ferricyanide (Figure 6b). Current densities were normalized to the CDW, to eliminate current variations caused by minor deviations in cell number between both conditions.

The current densities vary only slightly between CTAB treated cells and the control. In the first 24 h, CTAB treated cells reach minimal higher maximal current densities (1095.7 *vs.* 973.5 $\mu A\,g_{CDW}^{-1}\,cm^{-2}$), which cancels out during further cultivation, as the same charge is transferred after 120 h for treated and untreated cells. A similar effect is visible for oxidized ferricyanide concentration. With CTAB, slightly more ferricyanide is reduced, but at an identical rate. To rule out a concentration limitation for CTAB, another 20 μM of CTAB was added after 120 h for a final concentration of 40 μM CTAB. This, however, had a detrimental effect on the metabolism of the cells, resulting in an instant current decline. Moreover, an increased substrate uptake was not observed (data not shown).

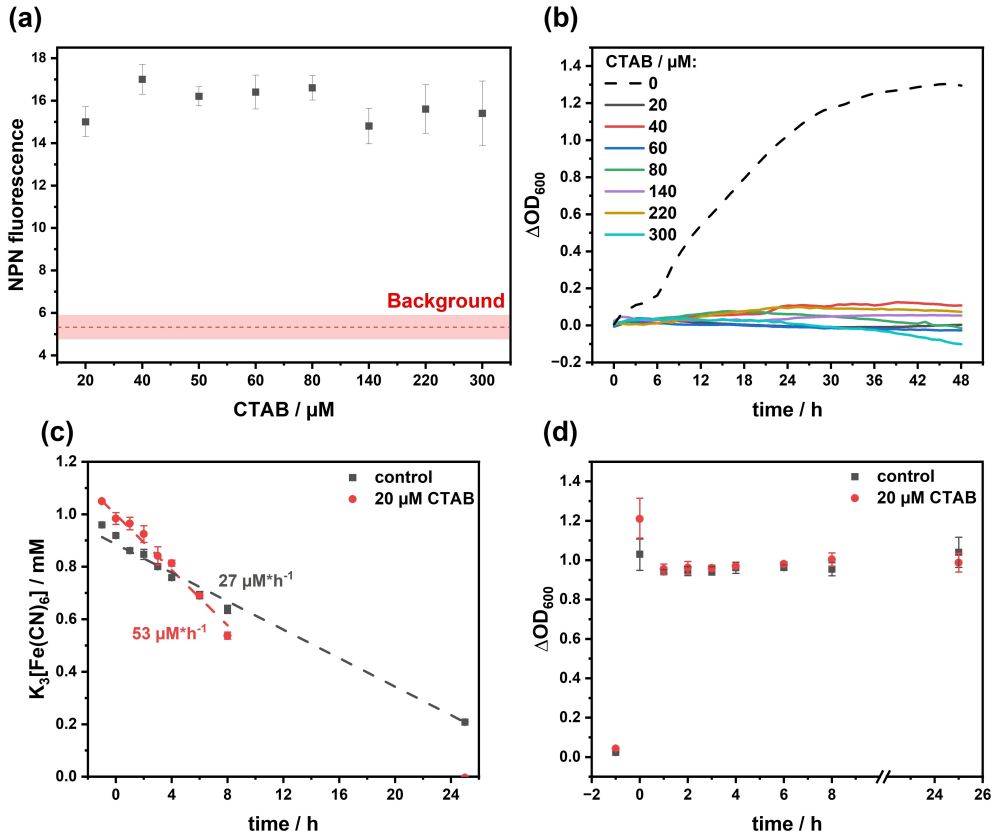

Figure 5. (a) NPN uptake assay with increasing CTAB concentrations with the background of NPN, buffer solution, and CTAB. (b) Growth analysis with increasing CTAB concentrations from a starting ΔOD_{600} of 0.5. (c) Reduction rates of ferricyanide with (red) and without (black) 20 µM of CTAB. (d) ΔOD_{600} of cultures reducing ferricyanide with and without CTAB. Conditions: MMasy minimal medium, 30 °C, anaerobic, n = 3. Error bars depict the standard deviation.

In conclusion, CTAB has a beneficial effect in low concentrations on the reduction rate of ferricyanide, but BES experiments suggest the effect is only minor. This opens up two hypotheses. Firstly, the natural membrane transfer of ferricyanide was not limiting the overall MET and secondly, the limitation must be in the metabolism or the interaction site, as enough oxidized mediator is provided during cultivation, excluding the anodic oxidation reaction as the limiting factor. Nevertheless, the first hypothesis stands against the obtained result of a faster reduction rate with CTAB in anaerobic serum flasks. The second hypothesis has to be further investigated e.g., via metabolic flux analysis.

Conclusions

Mediated extracellular electron transfer in *C. necator* via ferricyanide was characterized regarding the reduction site within the cell. Previous work by Nishio and co-workers[10] revealed higher expression levels of three nitrate reductases (NapD, NarK, NasD) when a polymeric ferrocene mediator transferred surplus electrons to an anode during aerobic cultivation. In this study, for the first time, expression rate analysis of hypothesized interaction sites, namely the nitrate and oxygen respiration chains, as well as the hydrogenases and three porins (OmpA, ImpK, czcC2) was performed in anaerobic BES reactors *vs.* aerobic cultivation conditions to elucidate on the ferricyanide reduction site(s). Furthermore, individual sites were specifically inhibited during BES cultivation with 5 mM ferricyanide mediating electrons to an anode as the sole terminal electron acceptor.

Inhibition with 5 mM azide hints towards cytochrome c oxidase as a reduction site due to an imminent decrease to 14% leftover current density after inhibition, consistent with the work of Ertl and Unterladstaetter[51] in *E. coli*. However, the specific inhibition with azide targeting the oxygen reduction site, which is not accessible for ferricyanide, results in an unclear mechanism for ferricyanide reduction. As demonstrated in the publication by Lai and co-workers,[14] cytochrome c reductase was found to be affected by antimycin A. However, an unclear side reaction of antimycin A prohibits ferricyanide oxidation by the anode. Therefore, the role of cytochrome c reductase in ferricyanide reduction remains questionable. The nitrate reductase NarG, also inhibited by azide, was proven to be present in BES cultures via qPCR and could also serve as reduction site for ferricyanide.

Comparing the megaplasmid deficient *C. necator* ΔpHG1 to the PHB^- strain in BES cultivations revealed that both strains can transfer electrons to ferricyanide, resulting in equal current densities. This excluded all hydrogenases present in *C. necator* from the list of potential interaction sites and further narrowed down the possible sites to respiration chain and nitrate

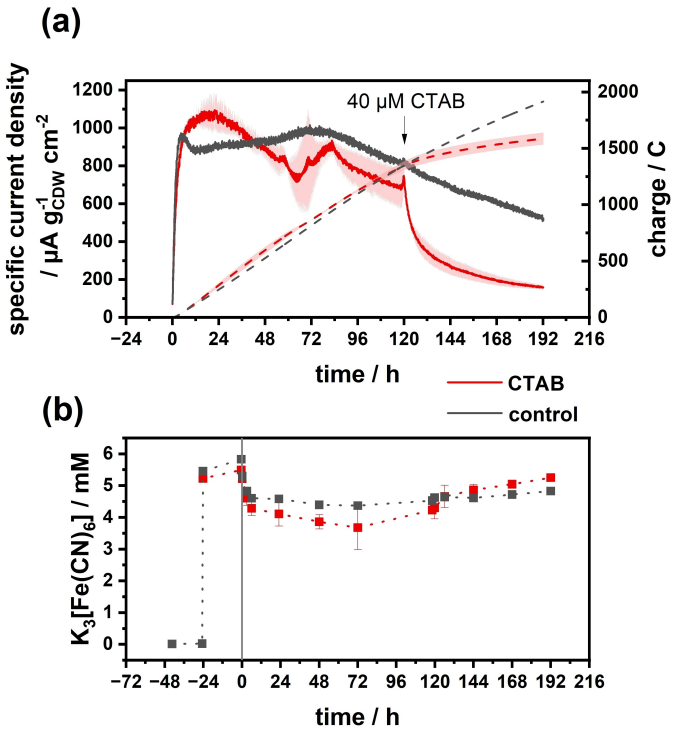

Figure 6. (a) specific current density normalized to CDW for BES cultures with 20 µM of CTAB (red, n = 3) and a control cultivation without CTAB (black, n = 1). Dashed lines indicate the charge transferred to the anode via ferricyanide. (b) concentrations of oxidized ferricyanide during BES cultivation with (red squares) and without (black squares) the addition of CTAB. Conditions: MMasy minimal medium, 30 °C, 400 rpm, pH 6.8, 500 mV *vs.* Ag/AgCl (satd. KCl). Error bars depict the standard deviation.

reduction proteins encoded on the chromosome. Of these, nitrite reductase (NirS) stood out as a possible candidate, catalysing a reaction with a redox potential close to that of ferricyanide alongside an observed 3.9 ± 1.1-fold expression under BES conditions. Furthermore, a 2.9 ± 0.6-fold overexpression *vs.* aerobic conditions of the porin OmpA was observed when cultivating *C. necator* under BES conditions. This might imply a ferricyanide transport property of this porin and opens up the possibility of enhancing ferricyanide membrane transfer. Alternatively, CTAB was applied as chemical permeabilizer to facilitate membrane transfer via artificial pores in the outer membrane. The reduction rate of ferricyanide was doubled with 20 µM CTAB added to the medium in anaerobic serum flasks. In contrast, the effect of CTAB was minor when applied in BES reactors and could not yield a higher charge transfer compared to untreated cells. Therefore, the hypothetical membrane transport limitation could not be eliminated via CTAB. Nevertheless, it cannot be ruled out that other mediators might benefit from chemical permeabilizers.

In a broader context, this study is a first step to elucidate MET for *C. necator* with one exemplary mediator. In future studies, whole transcriptome analysis comparing aerobic conditions to BES and autotrophic cultivations could reveal additional interaction sites, which have not yet been looked into.

Experimental Section

Bacterial Strains and Chemicals

Cupriavidus necator PHB^{-}4,[60] as well as *C. necator* HF210[61] (missing the pHG1 megaplasmid) were used in this study. All chemicals utilized in the study were procured from reputable suppliers, including Merck KGaA (Germany), VWR Chemicals (USA), Carl Roth GmbH & Co. KG (Germany), and Sigma Aldrich (USA).

Media and Culture Conditions

Cultures were incubated at 30 °C and 180 rpm in cultivation tubes containing 2.5 mL LB medium (10 g L^{-1} tryptone, 5 g L^{-1} yeast extract, 10 g L^{-1} NaCl). Cryo stocks were prepared by adding 25% glycerol to an exponential culture, which was subsequently frozen at −80 °C. For BES precultures, cryostocks were cultivated on LB agar plates (15 g L^{-1} agar) and incubated overnight at 30 °C. Liquid precultures were prepared by transferring a single colony into a 100 mL flask with baffles filled to 20 mL with LB. After 24 h, 1 L shake flasks with baffles filled to 200 mL with MMasy medium were inoculated with the exponential pre-culture to achieve an ΔOD_{600} of 0.1. The MMasy medium, as described by Sydow and co-workers,[62] consisted of 4 g L^{-1} fructose as the carbon and electron source, 2.895 g L^{-1} Na_2HPO_4, 2.707 g L^{-1} $NaH_2PO_4 \cdot H_2O$, 0.94 g L^{-1} $(NH_4)_2SO_4$, 0.8 g L^{-1} $MgSO_4 \cdot 7H_2O$, 0.097 g L^{-1} $CaSO_4 \cdot 2H_2O$, 0.17 g L^{-1} K_2SO_4, and 0.1% (v/v) of a trace element solution. The trace element stock solution was composed of 15 g L^{-1} $FeSO_4 \cdot 7H_2O$, 2.4 g L^{-1} $MnSO_4 \cdot H_2O$, 2.4 g L^{-1} $ZnSO_4 \cdot 7H_2O$, 0.48 g L^{-1} $CuSO_4 \cdot 5H_2O$, 1.8 g L^{-1} $Na_2MoO_4 \cdot 2H_2O$, 1.5 g L^{-1} $Ni_2SO_4 \cdot 6H_2O$, and 0.04 g L^{-1} $CoSO_4 \cdot 7H_2O$ dissolved in 0.1 M HCl. Cultures were then incubated in an orbital shaker at 180 rpm (2.5 cm orbit, Multitron, Infors, Bottmingen, Switzerland). The BES precultures were incubated for 48 h to ensure the stationary phase was reached before inoculating the reactor.

Autotrophic or anaerobic cultures were inoculated from liquid precultures in LB in gas-tight serum flasks (1000 mL). Each flask was filled to 200 mL with MMasy minimal medium without fructose. The headspace was then pressurized with the respective gas. For autotrophic conditions, a $H_2/CO_2/O_2$ gas mixture with a composition of 64:16:20 as described by Sydow and colleagues[62] was used. In the case of anaerobic cultivations with ferricyanide, 99.999% N_2 was applied. The gas phase was renewed after taking a sample.

Bioelectrochemical System

The BES reactor was used in the configuration already described before.[12] In brief, a polished graphite rod (Graphite 24, Germany) with a length of 80 mm and a diameter of 7 mm (geometrical surface area of 18 cm^2), held in place by a PTFE rod, served as the working electrode inside the 300 mL DASGIP stirred tank reactor. It was paired with a stainless-steel mesh electrode (1.4404, mesh size 0.1 mm, wire diameter 0.065 mm, Jaera GmbH + Co.KG, Germany) with a geometrical surface area of 20 cm^2, functioning as the counter electrode. The anodic and cathodic compartments were separated by a cation exchange membrane (Nafion117, QuinTech, Germany). The cathodic compartment, enclosed in a glass tube with one threaded side and an open side, held 10 mL of cathode buffer (28.95 g L^{-1} Na2HPO4, 27.07 g L^{-1} $NaH_2PO_4 \cdot$H2O). The anodic buffer consisted of MMasy medium with 4 g L^{-1} fructose as the substrate. The applied potential of 500 mV was controlled using a multi-channel potentiostat (MultiEmStat3 +, PalmSens, Netherlands) and Ag/AgCl (satd. KCl) reference electrodes (Xylem Analytics, Germany). 2 mL of ferricyanide was added as a concentrated stock solution (750 mM) for a final concentration of 5 mM. The anodic overpotential of 500 mV was applied to ensure

sufficient driving force for ferricyanide oxidation. pH control was achieved using pH sensors (Hamilton, Germany) along with Eppendorf DASGIP pH and pump modules, with 2.5 M NaOH being fed through the headspace of each reactor. This maintained a pH of 6.8 in the anodic compartment, while the cathodic chamber remained uncontrolled.

Analytics and Calculations

Culture broth samples were obtained from the reactors and subjected to centrifugation at 16,900 x g and 4 °C for 5 minutes. The resulting supernatant was filtered through a 0.2 μm PTFE filter. HPLC analysis was performed using an Agilent 1200 high-performance liquid chromatography system equipped with an Aminex HPX-87H column (Bio-Rad Laboratories GmbH, Germany). Concentrations of the substrate fructose were determined using a refractive index detector at 32 °C. The column temperature was maintained at 50 °C, and 5 mM H_2SO_4 at a flow rate of 0.5 mL min^{-1} was employed for isocratic elution of the analytes. Fructose standards ranging from 0.1 to 4 g L^{-1} in seven concentration steps were measured, and the corresponding areas were fitted using linear regression.

Determination of the redox state of the RM in the BES was performed as described before.[12,63] In short, the extinction of the characteristic wavelengths of ferricyanide (320/420 nm) were monitored offline with a spectrophotometer. Reduced ferricyanide does not absorb at 420 nm and can therefore be distinguished from the oxidized form. The concentrations were then determined via 7 standards of oxidized ferricyanide.

The coulombic efficiency (CE) was calculated via the following equation: CE [%] = $Q_{anode}/(Q_{substrate}-Q_{products})$*100. Q indicates the charge transferred to the anode in [C]. Fructose was used as the only substrate, contributing 24 equivalents of electrons per mol of fructose. Since no products were detected in culture supernatants, $Q_{products}$ was assumed to be 0.

RT-qPCR

Expression rates of the genes of interest encoding for possible mediator interaction sites were determined via qPCR. Analogous to qPCR reactions performed with *C. necator* mRNA in the literature, the housekeeping gene *gyrB* was used as positive control.[64] Cells were prepared immediately after taking samples from the cultures. Since all experiments were at least performed as triplicates, mRNA extraction was performed for each of those triplicates using the Monarch Total RNA miniprep Kit (T2010, NEB, USA), according to the manual for tough-to-lyse samples (available online). Here, an enzymatic lysis with 1 g L^{-1} lysozyme in 10 mM TRIS buffer (pH = 8.4) at 25 °C for 5 min was performed prior to adding monarch RNA lysis buffer. During the extraction, an on-column DNAse I treatment was performed to remove any residues of DNA. The transcription into cDNA was performed with a Luna® Universal One-Step RT-qPCR Kit (E3005, NEB, USA) with a total RNA concentration of < 0.05 g L^{-1}. The reaction setup was performed as described in the associated manual. Primers for the specific genes of interest are listed in (Table S1) The transcription as well as the qPCR reaction was done in an Agilent AriaMX qPCR system with the SYBR® scan mode. Relative gene expression rates were determined *vs.* aerobic control cultivations as calibrator using the $2^{-\Delta\Delta Ct}$ method.[65]

Supporting Information

The authors have cited additional references within the Supporting Information (Ref. [66,67]).

Acknowledgements

This work was created as part of the project "Bioelectrochemical and engineering fundamentals to establish electro-biotechnology for biosynthesis – Power to value-added products (eBiotech)", which is funded by the Deutsche Forschungsgemeinschaft (DFG, German Research Foundation) – Project number 422694804. Open Access funding enabled and organized by Projekt DEAL.

Conflict of Interests

The authors declare no conflict of interest.

Data Availability Statement

The data that support the findings of this study are available from the corresponding author upon reasonable request.

Keywords: Bioelectrochemical system · Cytochromes · Electron transfer · Mediator interaction · Respiratory inhibition

[1] R. R. Dalsasso, F. A. Pavan, S. E. Bordignon, G. M. F. de Aragão, P. Poletto, *Process Biochem.* **2019**, *85*, 12.
[2] T. Krieg, A. Sydow, S. Faust, I. Huth, D. Holtmann, *Angew. Chem. Int. Ed. Engl.* **2018**, *57*, 1879.
[3] S. Milker, A. Sydow, I. Torres-Monroy, G. Jach, F. Faust, L. Kranz, L. Tkatschuk, D. Holtmann, *Biotechnol. Bioeng.* **2021**, *118*, 2694.
[4] S. Milker, D. Holtmann, *Microb. Cell Fact.* **2021**, *20*, 89.
[5] J. Overhage, A. Steinbüchel, H. Priefert, *Appl. Environ. Microbiol.* **2002**, *68*, 4315.
[6] J. Lu, C. J. Brigham, C. S. Gai, A. J. Sinskey, *Appl. Microbiol. Biotechnol.* **2012**, *96*, 283.
[7] J. Panich, B. Fong, S. W. Singer, *Trends Biotechnol.* **2021**, *39*, 412.
[8] A. Tiemeyer, H. Link, D. Weuster-Botz, *Appl. Microbiol. Biotechnol.* **2007**, *76*, 75.
[9] E. Schwartz, A. Henne, R. Cramm, T. Eitinger, B. Friedrich, G. Gottschalk, *J. Mol. Biol.* **2003**, *332*, 369.
[10] K. Nishio, Y. Kimoto, J. Song, T. Konno, K. Ishihara, S. Kato, K. Hashimoto, S. Nakanishi, *Environ. Sci. Technol. Lett.* **2014**, *1*, 40.
[11] Y. H. Lai, J. C.-W. Lan, *Int. J. Hydrogen Energy* **2021**, *46*, 16787.
[12] A. Gemünde, E. Rossini, O. Lenz, S. Frielingsdorf, D. Holtmann, *Bioelectrochemistry* **2024**, *158*, 108694.
[13] A. Gemünde, J. Gail, D. Holtmann, *Electrochem. Commun.* **2024**, *162*, 107705.
[14] B. Lai, P. V. Bernhardt, J. O. Krömer, *ChemSusChem* **2020**, *13*, 5308.
[15] L. Gu, X. Xiao, G. Zhao, P. Kempen, S. Zhao, J. Liu, S. Y. Lee, C. Solem, *Microb. biotechnol.* **2023**, *16*, 1277-1292.
[16] R. Y. A. Hassan, U. Wollenberger, *Anal. Bioanal. Chem.* **2016**, *408*, 579.
[17] D. H. Park, J. G. Zeikus, *J. Bacteriol.* **1999**, *181*, 2403.
[18] S. Hintermayer, S. Yu, J. O. Krömer, D. Weuster-Botz, *Biochem. Eng. J.* **2016**, *115*, 1.
[19] C. Cai, B. Liu, M. V. Mirkin, H. A. Frank, J. F. Rusling, *Anal. Chem.* **2002**, *74*, 114.
[20] H. Teramoto, T. Shimizu, M. Suda, M. Inui, *Int. J. Hydrogen Energy* **2022**, *47*, 22010.

[21] B. E. Conley, M. T. Weinstock, D. R. Bond, J. A. Gralnick, *Appl. Environ. Microbiol.* **2020**, *86*, e01253–20.
[22] B. R. Ringeisen, E. Henderson, P. K. Wu, J. Pietron, R. Ray, B. Little, J. C. Biffinger, J. M. Jones-Meehan, *Environ. Sci. Technol.* **2006**, *40*, 2629.
[23] S. Ishii, K. Watanabe, S. Yabuki, B. E. Logan, Y. Sekiguchi, *Appl. Environ. Microbiol.* **2008**, *74*, 7348.
[24] J. Boonstra, H. J. Sips, W. N. Konings, *Eur. J. Biochem.* **1976**, *69*, 35.
[25] A. W. Confer, S. Ayalew, *Vet. Microbiol.* **2013**, *163*, 207.
[26] J. Shearer, D. Jefferies, S. Khalid, *J. Chem. Theory Output* **2019**, *15*, 2608.
[27] L.-S. Ma, J.-S. Lin, E.-M. Lai, *J. Bacteriol.* **2009**, *191*, 4316.
[28] J. D. Mougous, M. E. Cuff, S. Raunser, A. Shen, M. Zhou, C. A. Gifford, A. L. Goodman, G. Joachimiak, C. L. Ordoñez, S. Lory et al., *Science* **2006**, *312*, 1526.
[29] C. Rensing, T. Pribyl, D. H. Nies, *J. Bacteriol.* **1997**, *179*, 6871.
[30] C. G. Friedrich, B. Friedrich, B. Bowien, *J. Gen. Microbiol.* **1981**, *122*, 69.
[31] B. Friedrich, E. Heine, A. Finck, C. G. Friedrich, *J. Bacteriol.* **1981**, *145*, 1144.
[32] B. C. Berks, S. J. Ferguson, J. W. Moir, D. J. Richardson, *Biochim. Biophys. Acta* **1995**, *1232*, 97.
[33] B. Lai, S. Yu, P. V. Bernhardt, K. Rabaey, B. Virdis, J. O. Krömer, *Biotechnol. Biofuels* **2016**, *9*, 39.
[34] P. R. Alefounder, J. E. McCarthy, S. J. Ferguson, *FEMS Microbiol. Lett.* **1981**, *12*, 321.
[35] A. Pohlmann, R. Cramm, K. Schmelz, B. Friedrich, *Mol. Microbiol.* **2000**, *38*, 626.
[36] R. Cramm, A. Pohlmann, B. Friedrich, *FEBS Lett.* **1999**, *460*, 6.
[37] M. L. Fultz, R. A. Durst, *Anal. Chim. Acta* **1982**, *140*, 1.
[38] J. W. Moir, N. J. Wood, *Cell. Mol. Life Sci.* **2001**, *58*, 215.
[39] U. Warnecke-Eberz, B. Friedrich, *Arch. Microbiol.* **1993**, *159*, 405.
[40] L.-S. Huang, D. Cobessi, E. Y. Tung, E. A. Berry, *J. Mol. Biol.* **2005**, *351*, 573.
[41] G. von Jagow, P. O. Ljungdahl, P. Graf, T. Ohnishi, B. L. Trumpower, *J. Biol. Chem.* **1984**, *259*, 6318.
[42] T. Friedrich, P. van Heek, H. Leif, T. Ohnishi, E. Forche, B. Kunze, R. Jansen, W. Trowitzsch-Kienast, G. Höfle, H. Reichenbach, *Eur. J. Biochem.* **1994**, *219*, 691.
[43] N. Li, K. Ragheb, G. Lawler, J. Sturgis, B. Rajwa, J. A. Melendez, J. P. Robinson, *J. Biol. Chem.* **2003**, *278*, 8516.
[44] Z. Xi, J. Guo, J. Lian, H. Li, L. Zhao, X. Liu, C. Zhang, J. Yang, *Bioresour. Technol.* **2013**, *140*, 22.
[45] M. J. Fei, E. Yamashita, N. Inoue, M. Yao, H. Yamaguchi, T. Tsukihara, K. Shinzawa-Itoh, R. Nakashima, S. Yoshikawa, *Acta Crystallogr. Sect. D* **2000**, *56*, 529.
[46] D. J. Hyndman, Y. M. Milgrom, E. A. Bramhall, R. L. Cross, *J. Biol. Chem.* **1994**, *269*, 28871.
[47] A. Craske, S. J. Ferguson, *Eur. J. Biochem.* **1986**, *158*, 429.
[48] J. Simon, M. Sänger, S. C. Schuster, R. Gross, *Mol. Microbiol.* **2003**, *49*, 69.
[49] S. Dementin, P. Arnoux, B. Frangioni, S. Grosse, C. Léger, B. Burlat, B. Guigliarelli, M. Sabaty, D. Pignol, *Biochemistry* **2007**, *46*, 9713.
[50] E. Maklashina, G. Cecchini, *Arch. Biochem. Biophys.* **1999**, *369*, 223.
[51] P. Ertl, B. Unterladstaetter, K. Bayer, S. R. Mikkelsen, *Anal. Chem.* **2000**, *72*, 4949.
[52] M. S. Al-Abdul-Wahid, F. Evanics, R. S. Prosser, *Biochem.* **2011**, *50*, 3975.
[53] A. A. Konstantinov, T. Vygodina, N. Capitanio, S. Papa, *Biochim. Biophys. Acta* **1998**, *1363*, 11.
[54] N. Capitanio, G. Capitanio, D. Boffoli, S. Papa, *Biochem.* **2000**, *39*, 15454.
[55] M. Wikström, K. Krab, V. Sharma, *Chem. Rev.* **2018**, *118*, 2469.
[56] J. Liu, Y. Qiao, Z. S. Lu, H. Song, C. M. Li, *Electrochem. Commun.* **2012**, *15*, 50.
[57] Q. Wen, F. Kong, F. Ma, Y. Ren, Z. Pan, *J. Power Sources* **2011**, *196*, 899.
[58] J. Wu, Y. Li, X. Chen, N. Li, W. He, Y. Feng, J. Liu, *Sci. Total Environ.* **2022**, 822, 153443.
[59] I. M. Helander, H.-L. Alakomi, K. Latva-Kala, P. Koski, *Microbiol.* **1997**, *143*, 3193.
[60] H. G. Schlegel, R. Lafferty, I. Krauss, *Arch. Mikrobiol.* **1970**, *71*, 283.
[61] C. Kortlüke, B. Friedrich, *J. Bacteriol.* **1992**, *174*, 6290.
[62] A. Sydow, T. Krieg, R. Ulber, D. Holtmann, *Eng. Life Sci.* **2017**, *17*, 781.
[63] A. Gemünde, J. Gail, D. Holtmann, *Chemsuschem* **2023**, 16, e202300181.
[64] C. Windhorst, J. Gescher, *Biotechnol. Biofuels* **2019**, *12*, 163.
[65] K. J. Livak, T. D. Schmittgen, *Methods* **2001**, *25*, 402.
[66] A. J. Ruff, M. Arlt, M. van Ohlen, T. Kardashliev, M. Konarzycka-Bessler, M. Bocola, A. Dennig, V. B. Urlacher, U. Schwaneberg, *J. Mol. Catal. B* **2016**, *134*, 285.
[67] I. M. Helander, T. Mattila-Sandholm, *Int. J. Food Microbiol.* **2000**, *60*, 153.

Manuscript received: March 28, 2024
Revised manuscript received: April 30, 2024
Version of record online: June 27, 2024